ISSN No: 2348-4845
International Journal & Magazine of Engineering, Technology, Management and Research
A Peer Reviewed Open Access International Journal

Welding Simulations of Aluminum Alloy Joints Finite Element Analysis

Tummalapalli Krishna Chaitanya
M.Tech.(CAD/CAM),
Department of Mechanical Engineering,
Kakinada Institute of Technological Sciences,
A.Agraharam- Ramachandrapuram East Godavari District.

Mr.D.Vijaya Prasad
Associate Professor,
Department of Mechanical Engineering,
Kakinada Institute of Technological Sciences,
A.Agraharam- Ramachandrapuram East Godavari District.

ABSTRACT:

Simulations of the welding process for butt and tee joints using finite element analyses are presented. The base metal is aluminum alloy 2519-T87 and the filler material is alloy 2319. The simulations are performed with the commercial software SYSWELD+®, which includes moving heat sources, material deposit, metallurgy of binary aluminum, temperature dependent material properties, metal plasticity and elasticity, transient heat transfer and mechanical analyses. One-way thermo-mechanical coupling is assumed, which means that the thermal analysis is completed first, followed by a separate mechanical analysis based on the thermal history.The residual stress state from a three-dimensional analysis of the butt joint is compared to previously published results.

For the quasi-steady state analysis the maximum residual longitudinal normal stress was within 3.6% of published data, and for a fully transient analysis this maximum stress was within 13% of the published result. The tee section requires two weld passes, and both a fully three-dimensional (3-D) and a 3-D to 2-D solid-shell finite elements model were employed. Using the quasi-steady state procedure for the tee, the maximum residual stresses were found to be 90-100% of the room-temperature yield strength. However, the longitudinal normal stress in the first weld bead was compressive, while the stress component was tensile in the second weld bead. To investigate this effect a fully transient analysis of the tee joint was attempted, but the excessive computer times prevented a resolution of the longitudinal residual stress discrepancy found in the quasi-steady state analysis. To reduce computer times for the tee, a model containing both solid and shell elements was attempted.

Unfortunately, the mechanical analysis did not converge, which appears to be due to the transition elements used in this coupled solid-shell model. Welding simulations to predict residual stress states require three-dimensional analysis in the vicinity of the joint and these analyses are computationally intensive and difficult. Although the state of the art in welding simulations using finite elements has advanced, it does not appear at this time that such simulations are effective for parametric studies, much less to include in an optimization algorithm.The background for this work is presented in this chapter. Finite element analysis in the optimal design of vehicle structures is discussed in the context of a project on the weight reduction of a military assault vehicle. A technique called global/local optimization is summarized, which is a method to include the results of numerically intensive, detailed analyses in the overall design algorithm. In particular, the structural detail of interest is the welded aluminum joint. The assault vehicle has numerous welded joints, and the aim of this work is to explore the possibility of using the results from detailed welding simulations in the global-local optimization scheme.

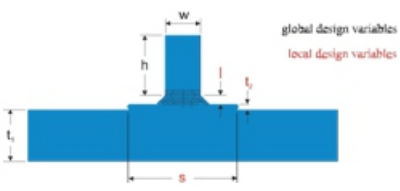

Advanced Amphibious Assault Vehicle (AAAV):

Typically large, and computationally intensive finite element models are utilized to predict the overall response of a structure, including important quantities such as stresses and displacements [2].

ISSN No: 2348-4845
International Journal & Magazine of Engineering, Technology, Management and Research
A Peer Reviewed Open Access International Journal

Moreover, repetitive analyses are required in design algorithms, and execution of many finite element analyses usually demands approximations to reduce run times. Therefore, it is typical for finite element models of the overall structure to have reduced detail which does not take into account local design issues. Unfortunately, many of the local design details that are neglected in the overall vehicle finite element analysis have a strong influence on the response and failure characteristics of the vehicle, and must be accounted for during overall design of the vehicle.

Global/Local Optimization:

An important objective in the optimization process of vehicle structural design is to reduce the weight of the vehicle without a failure of any kind occurring under service loads. However, the difficult issue is that of the level of detail to include in the finite element structural analysis to evaluate constraints. A method to include local design details early in the vehicle design process is called the global/local design methodology. A global/local optimization strategy for the overall design of complex structures such as the AAAV can account for the local details and their interaction with the global response of the vehicle. In the global/local approach, the overall design problem is decomposed into a global problem and a local problem. The global problem focuses on the design and analysis of the entire vehicle structure using simplified models, typically shell finite element models. At the global design level, the finite element model of the complete structure is used to compute the overall response of the structure and to assure that specified constraints on displacements and stresses are not violated.

Fig. 1.4 Finite Element Model of Local Weld Joint with Design Variables [2].

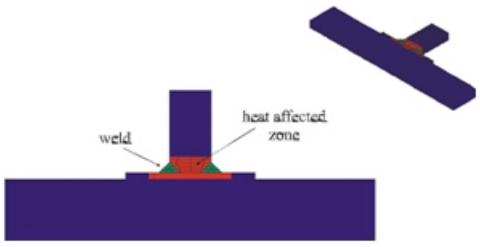

Fig. 1.5 Finite Element Model of Local Weld Joint depicting weld and heat affected zone [2]

arc is stepped along the remainder of the plate using a time step of 0.5s until a time of 50s. Element activation/de-activation was implemented for this part of the simulation. One element was activated ahead of the heat source, which corresponds to 3 mm ahead of the source. A transient analysis is required to capture the end effects of the weld arc leaving the plate. The temperature distribution at a time of 50s is shown in Figure 6.2. From t = 50s until 5000s, the heat source removed from the plate and the plate is allowed to cool. Ideally, the plate should cool to the ambient temperature of 20oC after a time of 5000s, yet using the convection coefficient reported by Michaleris et al. [14], the final temperature was 53oC. Other authors have reported higher convection coefficients by factors of 2-10 times those used here [46]. The final temperature upon cool-down is shown in Figure 6.3.

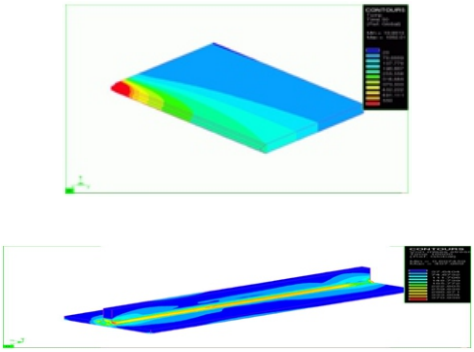

Fig. 6.2 Surface temperature distribution during the first weld pass of the butt joint model at t = 50s.

Now that the thermal history has been determined, the residual stress distribution is calculated. As described in Chapter 5, a mechanical analysis stage corresponding to each thermal analysis stage is completed. The final von Mises residual stress state after cool-down is shown in Figure 6.4. It is interesting to note that on the majority of the external surfaces the residual stresses are minimal, and it is not until after the part is sectioned are the highest residual stress.

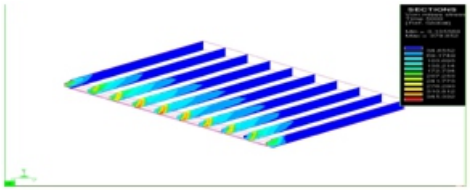

Fig. 6.4 Surface contours of the von Mises stress after the first weld pass of the butt joint model at t = 5000s

ISSN No: 2348-4845
International Journal & Magazine of Engineering, Technology, Management and Research
A Peer Reviewed Open Access International Journal

It is interesting to see the evolution of the longitudinal normal stress, σ yy , in cross sections of the plate normal to the welding direction. These stress distributions are shown in Figure 6.6, where the longitudinal normal stress is denoted as σ 22 in the legend. Contours of σ yy in the central cross section of the plate are shown in Figure 6.7. The stress distribution shown Figure 6.6 is similar to the distribution determined by Michaleris et al.[14], which is shown in Figure 6.8. The maximum value of σ yy is within 3.6% of the maximum reported in Ref.[14].

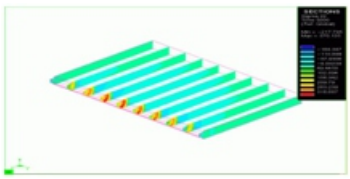

o complete the second weld pass, the transient analysis steps the weld arc from t = 5000s to 10000s using a time step of 0.5s. The temperature distributions at t = 5045s, 5050s, and 10000s are shown in Figure 6.21, Figure 6.22, and Figure 6.23, respectively.

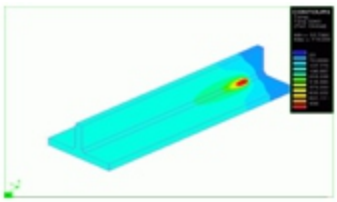

Fig. 6.21 Distribution of the surface temperatures for the second weld pass of the tee joint model at t = 5045s

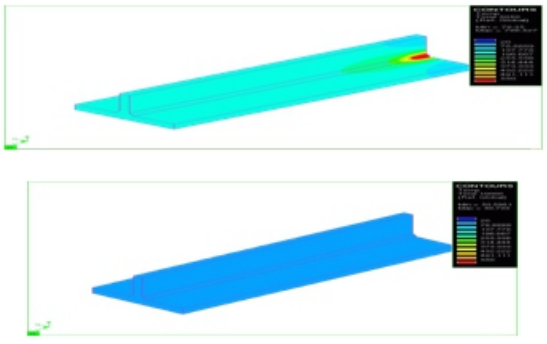

The phase 1 constitution after completion of the second weld pass is shown in Figure 6.26 and Figure 6.27. Again the change in phase 1 concentration is from about 40% to 95% in the second weld bead area, but the penetration of the weld zone into the joint from the second bead is not as great as is the penetration of the weld zone from the first pass. This lack of penetration of the second bead weld zone was due to the slightly lower temperatures the work piece experienced in the transient analysis for the second weld pass. In general, it was expected that the weld zone, and consequently the heat affected zone, would be much larger. This relatively small weld zone may be due to the fact that the metallurgical properties were estimated from the available literature. By adjusting the parameters of dissolution temperature Tr, the time to dissolution tr, the enthalpy of metastable solvus Qs, and the energy for activation of the diffusion process of the less mobile of the alloy elements Qd as described in Equation (2.1) on page 27, a larger heat affected zone could be produced. Unfortunately, the long computation times required for these analyses prevented further investigation into the metallurgical parameters.

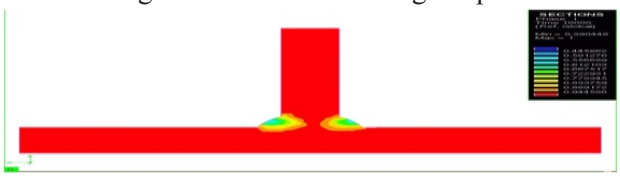

Fig. 6.27 Distribution of phase 1 material over the cross section after the second weld pass of the tee joint at t = 10,000s

After completion of the thermal analyses, the mechanical analyses were executed. The residual stress state was computed for the first weld pass and then the second weld pass. After cool-down of the first weld bead at t = 5000s, the von Mises residual stress state is computed and a surface contour plot of it is shown in Figure 6.28. The residual stresses on the surface are low, but the cross-sectional plots of the residul stresses shown in Figure 6.29 indicate that the highest.

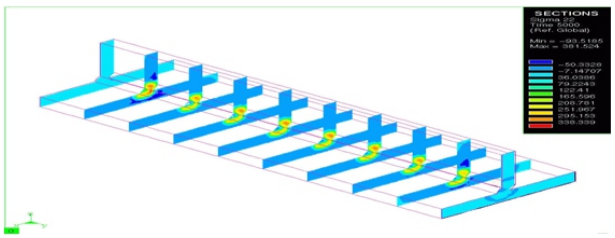

Fig. 6.31 Distribution of the longitudinal normal stress in several cross sections after the first weld pass of the tee joint at t = 5000s

The distribution of the longitudinal normal stress over several cross sections of the tee joint is shown in Figure 6.31. Again, after sectioning it is apparent that a steady-state condition is attained in the central cross sections of the work piece. The distribution of the longitudinal normal stress in a central cross section is shown in Figure 6.32. Examining this stress state we find the longitudinal

ISSN No: 2348-4845
International Journal & Magazine of Engineering, Technology, Management and Research
A Peer Reviewed Open Access International Journal

normal stress is tensile within the base plate material at the juncture of the two plates, Continuing on to the final stress state after the second weld bead has been deposited, the von Mises stress after cool-down is depicted in Figure 6.33. Sectioning the part as shown in Figure 6.34 again reveals the steady-state reached in the central cross sections of the work piece. The distribution of the residual stress state in the central cross section is shown in Figure 6.35. Examining the stress state in this central cross section, notice that the peak magnitudes are as high as 370 MPa, which is just below the yield strength of 400 MPa.

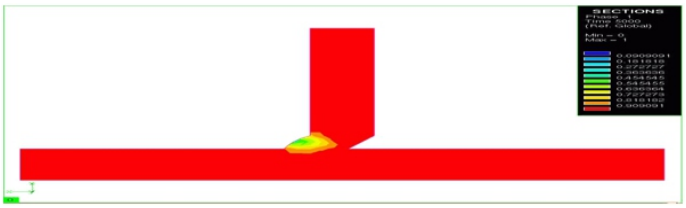

Fig. 6.41 Distribution of the phase 1 material from the transient analysis of the tee joint after the first weld pass at t = 5,000s.

The temperature distributions for the second weld bead would be the same as those found during the "moving reference frame" simulation, since they actually are the result of the transient second weld bead deposition. Consequently, the second weld bead analysis was not carried out.

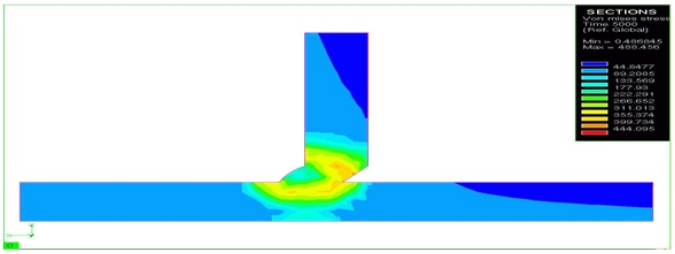

Fig. 6.44 Distribution of the von Mises stress in the central cross section from the transient analysis of the tee joint at t = 5000s.

The evolution of the longitudinal normal stress in several cross sections along the work piece is depicted in Figure 6.45. This distribution is much different than that predicted by the "moving reference frame" computation, which was shown Figure 6.31. The longitudinal normal stress distribution in the central cross section of the work piece from the transient analysis after the first weld pass is shown in Figure 6.46. Clearly, the distribution from the transient analysis different than predicted by the "moving reference frame" analysis, which was shown in Figure 6.32. The normal stress in the weld bead is tensile compared to the compressive stress predicted by the "moving reference frame" computation.

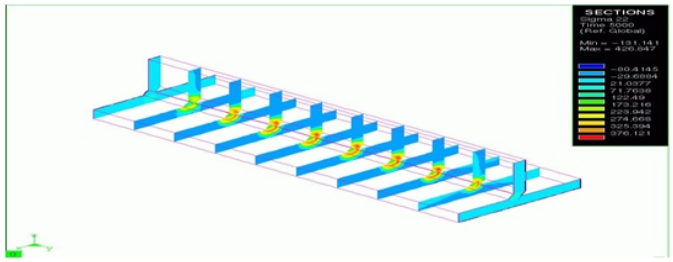

Fig. 6.45 Distribution of the longitudinal normal stress in several cross sections from the transient analysis of the tee joint at t = 5000s

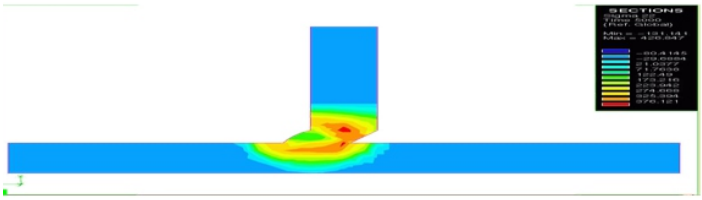

Fig. 6.46 Distribution of the longitudinal normal stress in the central cross section from the transient analysis of the tee joint at t = 500

6.3 Solid-Shell Coupled Tee Section Analysis:

Since the computation times were very large for the solid tee section model, especially for the fully transient analysis, a solid-shell coupled model was analyzed. The solid-shell model consists of solid elements in the weld zone and shell elements outside the joint. Transition elements are used to connect the solid and shell elements. A "moving reference frame" analysis was used forThe reason for undertaking the second analysis was that the element activation/de-activation function could not be utilized for the moving reference frame analysis. Bead deposit is an important aspect of welding, and therefore plays an important part in a finite element simulation of welding. Though the maximum longitudinal residual stress value was over-predicted by 13%, this could be caused by many factors. Michaleris et al. [14] used run-off tabs or extra material at the start and stop of the welded part to eliminate start and stop effects. Also, the mechanical boundary conditions could have varied since these were not published by Michaleris et al. [14]. Concluding, both analysis methods, moving reference frame and transient, provided results close to published results and confidence in using the SYSWELD software.

ISSN No: 2348-4845
International Journal & Magazine of Engineering, Technology, Management and Research
A Peer Reviewed Open Access International Journal

Table 7.1 Butt-weld Results

Analysis	Maximum Longitudinal Normal Stress
"Moving Ref. Frame"	370 MPa
Fully Transient	435 MPa
Michaleris et al. [14]	384 MPa

Conclusions

This research effort was successful in determining the weld heat affected zone and final residual stress state for a tee section joint and a butt-weld joint using finite element simulations. The butt-weld joint was the first simulation to be completed since results published by other authors [14] were readily accessible. After successful completion of butt-weld simulations which consisted of a single weld pass, the two weld pass tee section weld simulations were undertaken. The complexity of the tee section weld simulations were increased compared to the single pass butt-weld simulations due to the addition of the second weld pass. Multiple weld pass simulations require fully transient analyses which are computationally expensive and which prohibit quasi-steady state analyses.

Bibliography:

[1]General Dynamics Land Systems Programs. Advanced Amphibious Assault Vehicle [Online]. Available: http://www.gdls.com [2001, January].

[2]Ragon, S., Nikolaidis, E., Kapania, R., Johnson, E., and Gurdal, Z., 1999, "Global/Local Methodology for Optimum Design of AAAV Structures: Final Report", Department of Navy Contract: N00014-99-M-0253, pp. 1-37.

[3]Callister, W., Jr., 1995, Materials Science and Engineering, John Wiley & Sons, Inc., New York, NY, pp.236-243,142,558,560.

[4]Masubuchi, K., 1980, Analysis of Welded Structures-Residual Stresses, Distortion, and Their Consequences, Pergamon Press, New York, NY, pp. 20